Metallurgical
Science and Technology

A journal published
by Teksid Aluminum
twice a year

Vol. 21 No. 2, December 2003

LASER BEAM WELDING OF CAST COMMERCIAL PURE TITANIUM

S. Missori*, F. Murdolo, A. Sili****
***Dipartimento di Ingegneria Meccanica Università di Roma-Tor Vergata**
****Dipartimento di Chimica Industriale e Ingegneria dei Materiali Università di Messina**

LASER BEAM WELDING OF CAST COMMERCIAL PURE TITANIUM

S. Missori*, F. Murdolo, A. Sili****
***Dipartimento di Ingegneria Meccanica Università di Roma-Tor Vergata**
****Dipartimento di Chimica Industriale e Ingegneria dei Materiali Università di Messina**

Abstract

In this work the joining by Laser Beam Welding (LBW) technique of commercial pure Titanium (CP Ti) cast specimens was carried out. The specimens considered for welding trials were cylindrical and flat (parallelepiped shape) ingots of little dimensions, as utilised in dentistry applications. The welds were investigated by optical and scanning electron microscopy (SEM) and by X-ray diffraction (XRD) measurements; mechanical properties were experimented by Vickers microhardness, across traverses through the welded sections, and by tensile tests, performed, for comparison, also on unwelded specimens in as cast condition; fractured surfaces after tensile tests were observed by SEM.

Riassunto

In questo lavoro è stata messa a punto una tecnica di saldatura mediante fascio laser di campioni in titanio commercialmente puro. Per le prove di saldature sono stati considerati lingotti cilindrici e piani (di forma parallelepipeda), aventi piccole dimensioni come in uso in campo dentistico. I giunti saldati sono stati studiati attraverso osservazioni di microscopia ottica ed elettronica in scansione e misure di diffrazione dei raggi X; le proprietà meccaniche sono state sperimentate mediante misure di microdurezza Vickers, effettuate sulle sezioni saldate lungo direzioni trasversali, e mediante prove di trazione realizzate, per confronto, anche su campioni non saldati nelle condizioni di getti; le superfici di frattura ottenute con le prove di trazione sono state osservate mediante microscopia elettronica in scansione.

INTRODUCTION

Titanium and its alloys are successful materials due to their excellent corrosion resistance and strength to weight ratio. High strength Ti alloys are used in high performance applications such as chemical and power generation plants or aerospace industry [1,2]; cast CP Ti is widely used as an orthopaedic and dental implant material, because of its biocompatibility and relatively low cost [3]. For dental restorations, to eliminate the potential hazard of galvanism between endosseous Ti implants and frameworks in the oral cavity, it has been advocated to fabricate them with the same material [4]. Such an approach often entails Ti restorations are joined after casting by welding techniques.

Titanium and its alloys can be welded by a variety of conventional processes, although the Ti chemical reactivity requires special precautions to avoid contamination of the welded zone (WZ) and reduce the extension of the heat affected zone (HAZ). Fusion welding of Ti is performed principally in inert gas shielded arc processes [5], but also other processes have been developed, such as electron beam, because the high vacuum inside the welding chamber shields hot metal from contamination [6].

During the past decade, the use of LBW has increased in dentistry [6,7]. Since laser energy can be concentrated on a small area, there are little effects of heating and oxidation on the area surrounding the melting pot. The factors affecting mechanical properties of the welds are the nature of metals and the laser beam parameters [8]. The output energy, pulse duration and spot diameter can be adjusted to optimise the penetration depth of the laser beam according to the base metal used, because the rate of laser beam absorption, thermal conductivity and melting point are different in each metal. In general, it can be said that the greater the rate of laser beam absorption and the lower the thermal conductivity, the greater the penetration depth. Among dental metals, Titanium has a great rate of laser beam absorption and, in particular, a low thermal conductivity (0.17 W cm^{-1} $°C^{-1}$) which is approximately 1/20 of the conductivity of noble metals such as Au and Ag. These physical properties make Titanium particularly suitable to LBW, obtaining joints with tensile strength close to that of unwelded specimen, as pointed out in a previous work [9].

In this work welds of CP Ti for dental applications were obtained by a LBW procedure. The joints were investigated by metallography and mechanical tests. The microstructure characterisation was carried out by optical and scanning electron microscopy and by X-ray diffraction observations; Vickers microhardness and tensile tests were performed to evaluate mechanical properties of welds and, for comparison, on unwelded specimen, in as cast condition; fractured surfaces after tensile tests were observed by SEM.

MATERIALS AND METHODS

A number of samples of CP Ti ASTM grade 4 were produced according to manufacturer recommendations with a lost-wax procedure.
The samples were produced as cylindrical ingots (6 mm maximum diameter and 32 mm maximum length) for tensile test and as parallelepiped ingots (20 mm length, 5 mm width and 2 mm thickness) for metallograpy, XRD and hardness test, which require flat surfaces. After casting each specimen was sandblasted in order to remove the external layer of oxide and submitted to radiographic examination to reveal the presence of porosity and to discard defective specimens, if any.
The cylindrical samples to be welded were cut in two halves that were bevelled with an angle of 45° along conical surfaces and butted at the vertex. Flat samples were prepared with square edge for butt-welding procedure.
The LBW apparatus was type Orotig 60L, using yttrium, aluminium and garnet (YAG) crystals doped with neodymium (Nd) and dental pulsed. The focal radius of the laser beam was 0.6 mm; the pulse duration was 0.005 s, with an average power of 7.7 J. The inert gas for protection and control of plasma was argon with a flow rate of 0.2 dm^3/s.
A filler metal rod, diameter 1 mm, made of CP Ti Grade 1, was utilised. The impurity limits of both base and filler material are given in table 1, according to ASTM specifications.
Flat samples were metallography prepared, by conventional mechanical grinding and chemical etching, for optical and SEM observations, XRD measurements and Vickers microhardness tests.
The etchant utilised was the Kroll's solution (10 ml HF, 30 ml HNO_3 and 50 ml H_2O).
The scanning electron microscope was of type JSM-5600LV, operating at an accelerating voltage of 20 kV. The X-ray diffractometer was a Philips APD 2000 apparatus with CuKa radiation, that operated at 40 kV and 30 mA, the scanning rate being 0.04 $2\theta\ s^{-1}$, from $2\theta = 20°$ to $2\theta = 160°$.
Vickers microhardness tests (25 g load and 10 s time) were performed across traverses through the welded section, in order to obtain hardness profiles vs. the distance from the joint axis. For tensile tests, cylindrical samples, both welded and unwelded, with geometry according to ISO 6871 specifications (fig. 1), were utilised. Broken ends were submitted to fractographic examinations by SEM.

Table 1. Impurity maximum limits (weight %) of CP Ti base and filler materials.

Material	Ti grade	N	C	H	O	Fe
Base metal	4	0.05	0.10	0.015	0.40	0.50
Filler metal	1	0.03	0.10	0.015	0.18	0.20

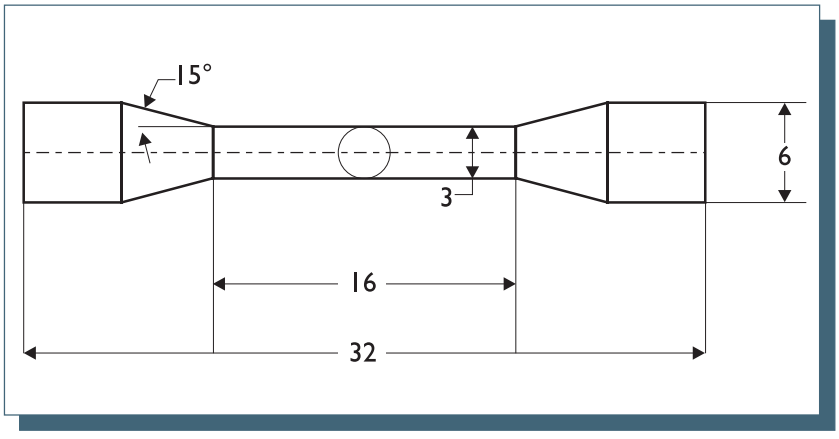

Fig. 1: Sketch of tensile test specimen, according to ISO 6871 Specification (dimensions in mm).

RESULTS AND DISCUSSION

Metallography

The base material microstructure is inhomogeneous and characterised by coarse grains, irregularly outlined, with large size (about 500 μm), as shown in fig. 2. Inside the grains, parallel striations, that can be ascribed to α platelets with the same orientation, are present. XRD analysis shows diffraction peaks of the a structure, without evidence of β structures peaks.
As known, pure titanium solidifies at 1668°C in a body-centred cubic structure (β crystal), that transform, below a transus temperature, to a hexagonal closed-packed structure (α crystal). Impurity elements can be α

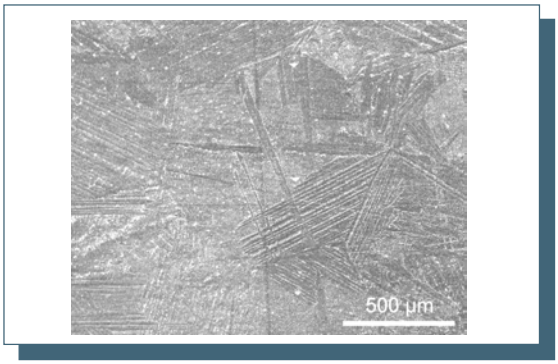

Fig. 2: Base material microstructure.

or β stabilisers: their contents influence the transus temperature value (888°C in ASTM grade 1 and 950°C in ASTM grade 4 pure titanium, with an uncertainty of about ± 15°C). A β structure cannot be retained at low temperature in unalloyed titanium, except in small quantities in materials containing β stabilising contaminants, such as iron. The microstructure of titanium at room temperature depends strongly on chemistry and cooling rate from β region. The β crystals can decompose by diffusion, through nucleation and growth, or by diffusionless processes (martensitic transformation). The first case gives structures of α platelet colonies of various morphology, characterised by spacing which decreases as cooling rate increases [10]; in the second case, α' martensite forms, that has the same crystal structure of the α phase, but exhibits lath or acicular morphology, depending on alloying or impurity contents [5].

The WZ, very narrow (400 – 500 μm width), is divided from the base metal by a fusion line that follows the grain boundaries of the base material; the WZ morphology is characterised by families of platelets inclined with respect to fusion line (fig. 3). Martensitic structures were not observed. The platelet spacing in WZ is finer than in base material, due to the high solidification rate of the melting pot produced by laser beam.

Near the fusion line, the base material affected by the thermal cycles of welding has a plate-like structure, with no evidence of other structural changes. The extension of this region, that is the HAZ, is comparable to the width of the WZ.

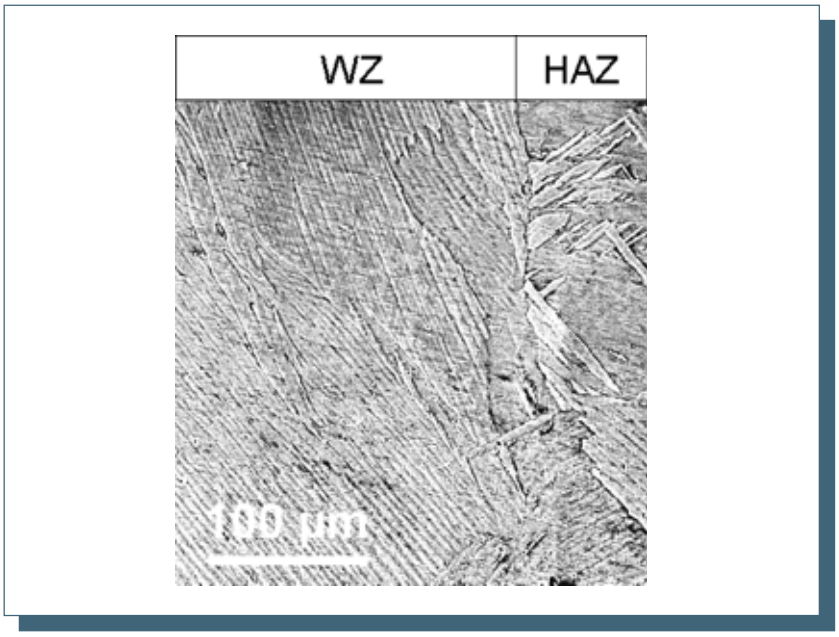

Fig. 3: Microstructure of WZ and HAZ.

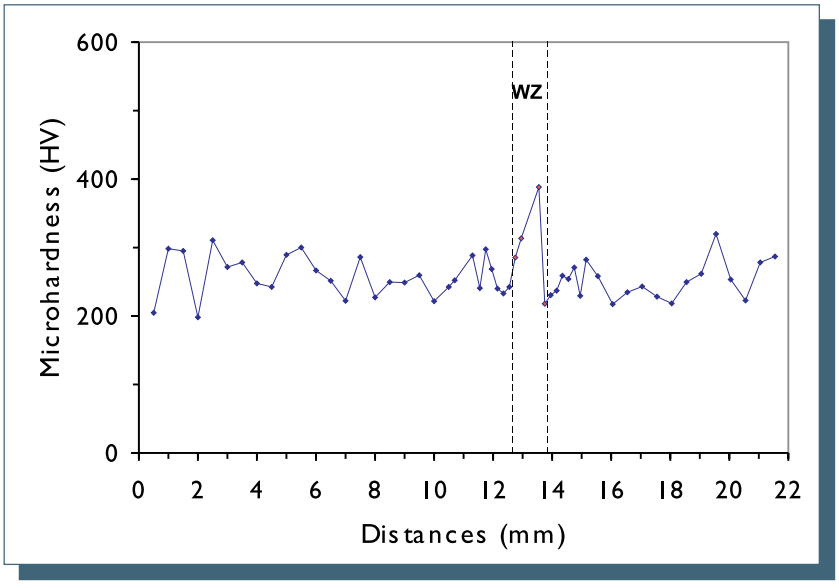

Fig. 4: Vickers microhardness profile along a traverse across welded joint.

Mechanical tests

The results of microhardness survey are given in fig. 4 for a representative traverse across welded joint. This traverse passes through the base material, the HAZ and the WZ. The microhardness data of base material are scattered around 250 HV, with a standard deviation of 67 HV, as the indentation size was less than grain size; the highest hardness values, with a peak around 350 HV, are recorded in the WZ, due to the observed finer width of platelets. Near the fusion line, at the base material side, the microhardness profiles do not show remarkable changes, giving no useful indication about the HAZ.

The results of tensile tests are reported in table 2; average (μ) and standard deviation (σ) values are given for tensile strength and elongation. Tensile

Table 2. Results of tensile tests for unwelded and welded specimens (average value μ; standard deviation σ).

	Elongation (%)		Tensile strength (MPa)	
	μ	σ	μ	σ
Unwelded specimens	9.5	0.1	593	10
Welded specimens	6.8	1.2	548	13

Fig. 5: Fractography of an unwelded specimen broken by tensile test: overall view.

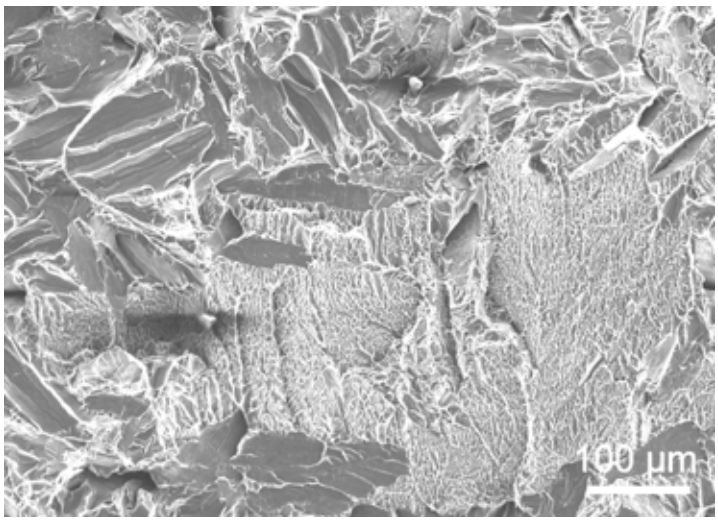

Fig. 6: Detail of cleavage planes in the fractured surface of fig. 5.

strength values are quite homogeneous for both welded and unwelded specimens, with little values of standard deviations. All the welded specimens fractured in the WZ with a tensile strength average value close to that of the base material, because only a reduction equal to 7.5% was recorded; instead, percent elongation underwent an appreciable reduction after welding. Its average value becomes equal to 71% of the percent elongation average value measured in the base material.

In figures from 5 to 8, some micrographs, obtained by SEM observation on broken ends of both unwelded and welded specimens, are reported. The overall view of broken ends of an unwelded specimen (fig. 5) shows a prevalently brittle fracture, characterised by crystallographic planes of cleavage (fig. 6).

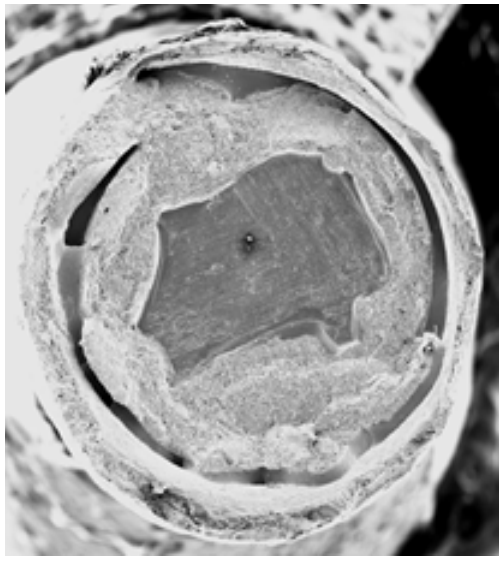

Fig. 7: Fractography of a welded specimen broken by tensile test: overall view.

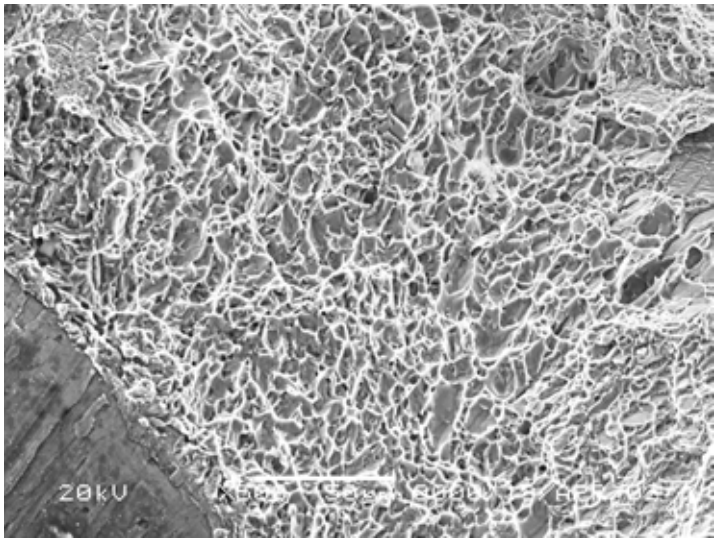

Fig. 8: Detail of dimples near the central cleavage zone in the fractured surface of fig. 8.

In welded specimens, the fractured surfaces, which are in the WZ, show distinct portions with brittle and ductile aspect (fig. 7). Some lack of fusion is observable, which reduces the overall strength of samples. The cleavage aspect prevails in the central area of the broken ends, while the dimple configuration is mainly distributed along an annular external area (fig 8).

CONCLUSIONS

The results of the present work can be summarised as follow:

1. satisfactory welds can be obtained by a LBW procedure on specimens of CP Ti of little dimensions, as occur in dentistry applications, except for some occasionally defects such as lack of fusion;
2. the metallographic investigations showed an a polycrystalline structure, characterised by coarse grain with platelet morphology;
3. in WZ and HAZ, both very narrow if compared to the specimen dimensions, no relevant structural changes took place; in any case the WZ showed a finer platelets spacing resulting in higher hardness values;
4. in welded samples mechanical properties were satisfactory, even if some loss of ductility respect to the base material is observed

REFERENCES

1. Boyer R.R. An overview of the use of titanium in the aerospace industry. *Materials Science and Engineering.* A213, (1996), 103-114
2. Gorynin I.V. Titanium alloys for marine application. *Materials Science and Engineering.* A263, (1999), 112-116
3. Kasemo B. Biocompatibility of titanium implants: surface science aspects. *J. Prosthet Dent.* 49 (1983), 832-837
4. Roggensack M., M.H Walter, K.W. Boning. Studies on laser and plasma welded titanium. *Dental Materials.* 9, (1993), 104-107
5. Wiskot Ansel H.W., T. Doumas, S.S. Scherrer, U. C. Belser. Mechanical and structural characteristics of commercially pure grade 2 Ti welds and solder joints. *J. of Materials Science: Materials in Medicine.* 12, (2001), 719-725
6. Qi Yunlian, Deng Ju, Hong Qun, Zeng Liying. Electron beam welding, laser beam welding and gas tungsten arc welding of titanium sheet. *Materials Science and Engineering.* A280, (2000), 177-181
7. Togaya T., T. Shinosaki. Introduction to laser welding in dentistry. *Quint Dent Tech.* 24 (6), (1999), 42-51
8. Liu J., I. Watanabe, K. Yoshida, M. Atsuta. Joint strength of laser-welded titanium. *Dentals Materials.* 18, (2002), 143-148
9. Missori S., A. Sili, "Mechanical properties of laser welded cast commercial pure titanium joints for dental applications", 7th European Conference on Advanced Materials and Processes - EUROMAT 2001, Rimini, 10-14 June 2001
10. Gil F.J., M.P. Ginebra, J.M. Manero, J.A. Planell. Formation of a-Widmanstätten structure: effects of grain size and cooling rate on the Widmanstätten morphologies and on the mechanical properties in Ti6Al4V alloy. *J. of Alloys and Compounds.* 329, (2001), 142-152